

ANALYSES OF COHERENCE AND DEFORMATION USING LAGRANGIAN AVERAGES



Marko Budišić
Igor Mezić (PI)

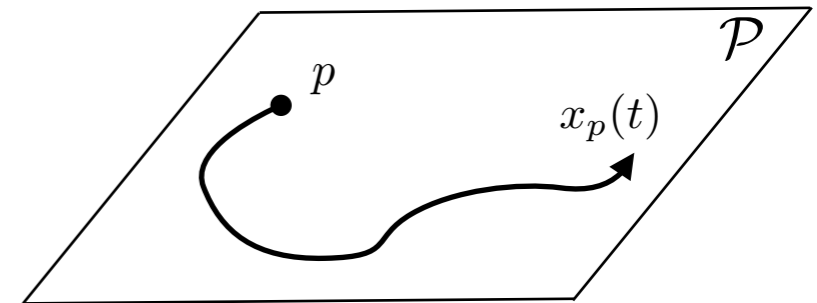
ONR MURI Ocean 3D+1
May 1, 2013

Both analyses use Lagrangian averaging, but applied to different fields.

Lagrangian trajectory:

$$\dot{x}_p = u(t, x_p), \quad x_p(0) = p$$

$$(p, t) \mapsto x_p(t)$$



Lagrangian average:

$$\tilde{f}(p, T) := \frac{1}{T} \int_0^T f(\tau, x_p(\tau)) d\tau$$

Initial
condition

Averaging
Interval

Choice of the field(s)
to be averaged

I. Ergodic Quotient: Coherent Structures

A (large) number of **stationary scalar fields**, related to the domain, not dynamics, e.g., spatial Fourier harmonics.

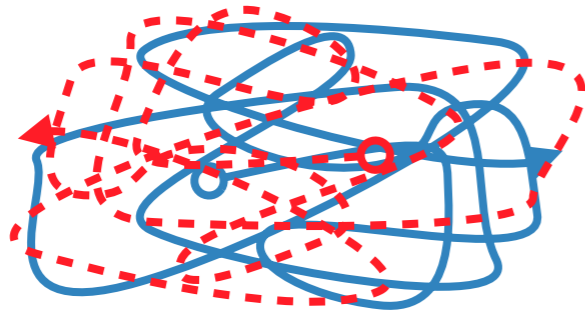
$$f(t, x) = f_k(x), \quad k = 1, 2, \dots$$

II. Mesochronic Analysis: Material Deformation

Fluid velocity field:
a single non-stationary vector field.

$$f(t, x) = u(t, x)$$

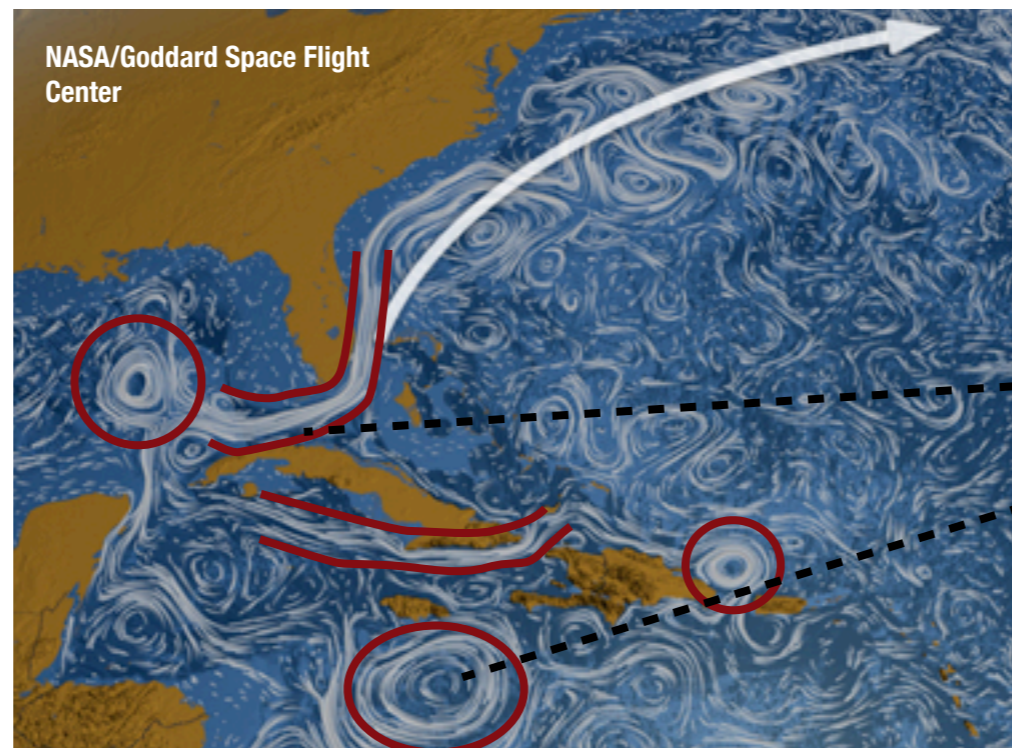
Quantifying trajectory similarity is difficult pointwise, but feasible using Lagrangian averages.



Comparison of tracer paths can be misleading: Two trajectories in a mixing region can never be aligned pointwise, but **on average** they have the same behavior.

Approach: compare tracers according to averages of many different scalar fields.

Result: we can **quantify** when trajectories are **equal** on average, but also when they are **similar** on average.

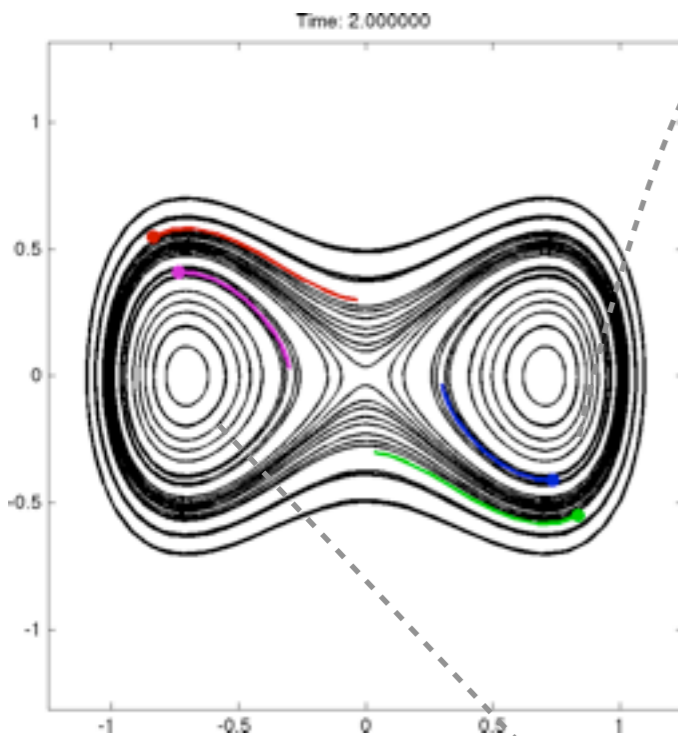


Layering: neighboring fluid parcels behave similarly

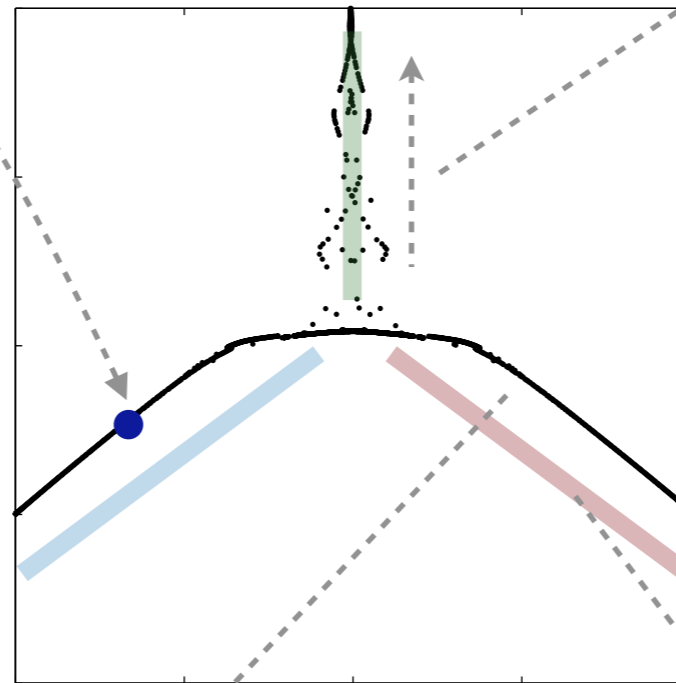
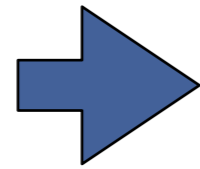
Ergodic quotient coordinates can be used to visualize coarse-grained flow patterns.

Entire trajectories mapped to single points.

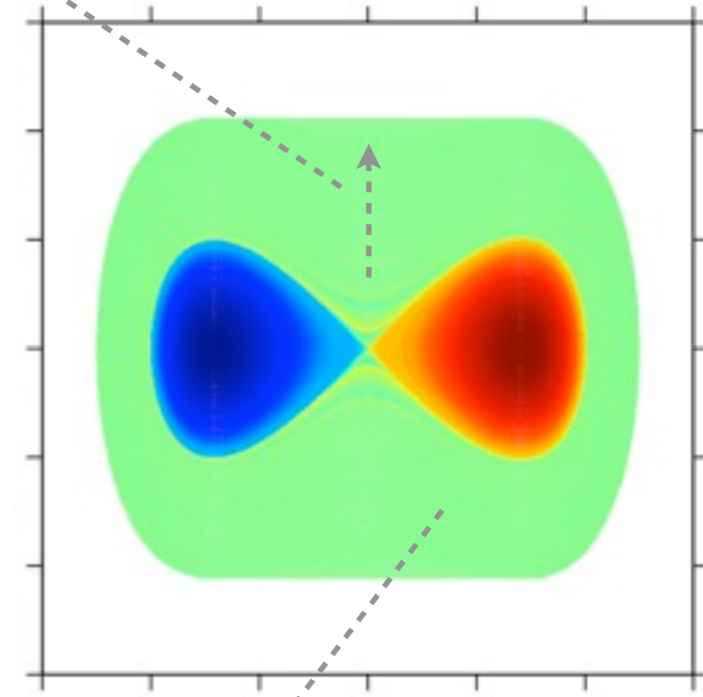
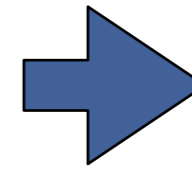
Axes in EQ act as generalized energies or stream functions.



Tracer paths



Ergodic Quotient



Colored initial conditions

Connected segments in EQ correspond to families of similar tracer paths.

Coloring initial conditions according to membership in connected segments visualizes coarse patterns.

[Budisic, Mezic
Physica D, 2012]

Trajectory curve description is replaced by vectors of Lagrangian averages.

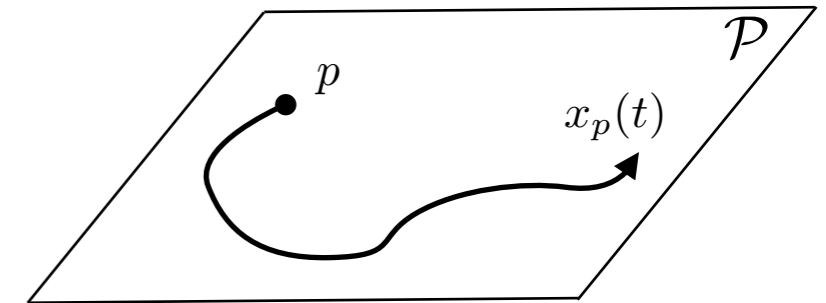
Curves:

$$\dot{x}_p = u(t, x_p), \quad x_p(0) = p$$

$$(p, t) \mapsto x_p(t)$$

Lagrangian averages of scalar fields:

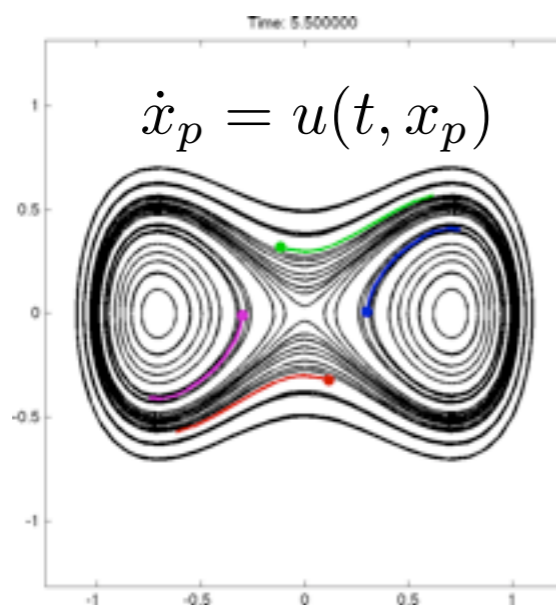
$$\tilde{f}(p, T) := \frac{1}{T} \int_0^T f(\tau, x_p(\tau)) d\tau$$



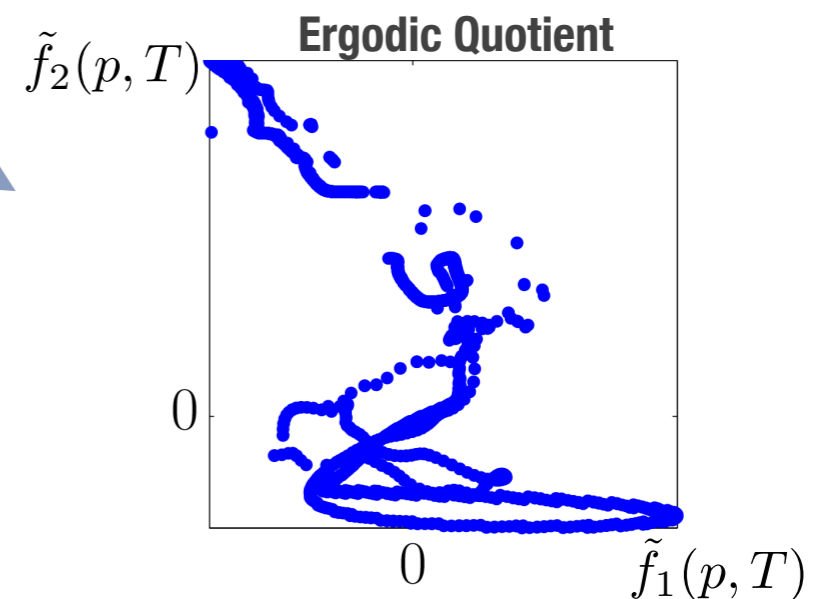
Ergodic quotient map is obtained by averaging a basis of continuous functions (scalar fields on the state space):

$$f_k(x) = e^{ik \cdot x}$$

$$(p, T) \mapsto \begin{bmatrix} \tilde{f}_1(p, T) \\ \tilde{f}_2(p, T) \\ \vdots \end{bmatrix}$$



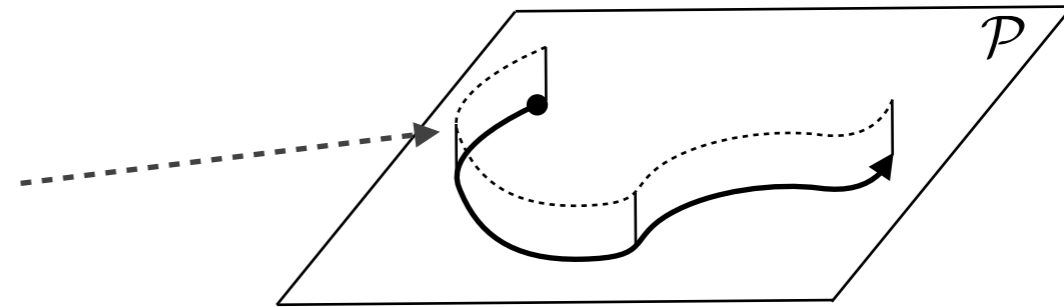
Representation of the tracer path portrait using averages of scalar fields.



Averaged scalar fields used as coordinates quantify “on-average” similarity between tracer paths.

If scalar fields are chosen as Fourier harmonics,
the Lagrangian **averages** are
spatial Fourier coefficients of averaging distributions.

$$f_k(x) = e^{ik \cdot x}$$

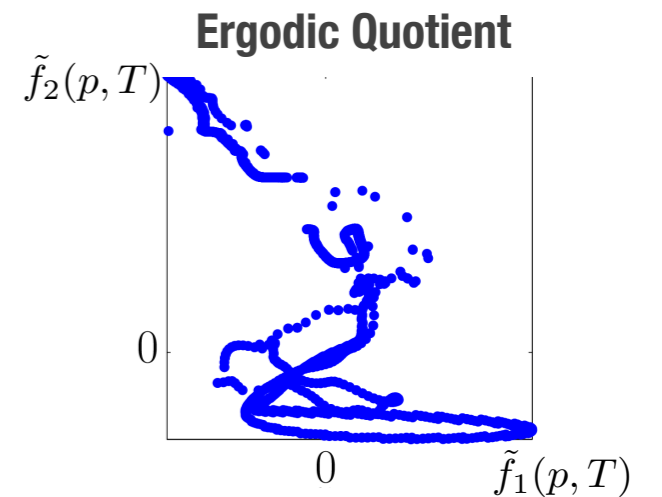


Continuous topology: Sobolev space norm.

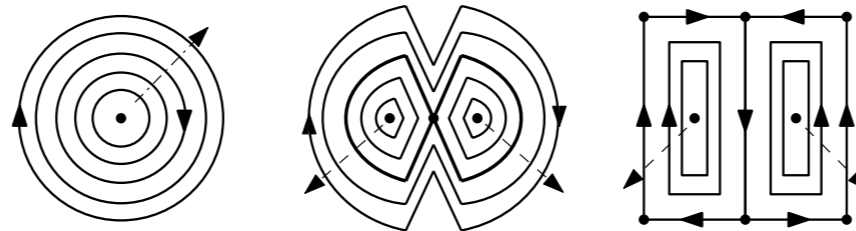
$$d_T(p_1, p_2)^2 = \sum_{k \in \mathbb{Z}^d} \frac{|\tilde{f}_k(p_1) - \tilde{f}_k(p_2)|^2}{(1 + |k|^2)^s}$$

Wavevectors

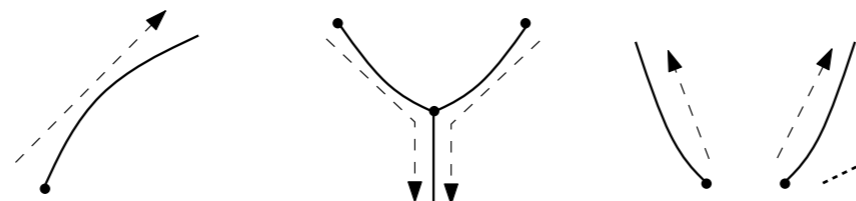
Acts as a low-pass filter:
de-emphasizes
small scale differences.



Tracer trajectories



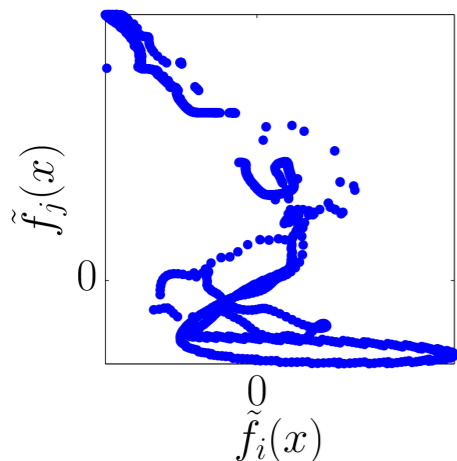
Ergodic Quotient
(in cts. topology)



Stagnation points on
separatrices prevent
ergodic quotient from
connecting.

Diffusion maps are a nonlinear coordinate reduction preserving the intrinsic geometry of the Ergodic Quotient (EQ).

EQ: Averaged Fields

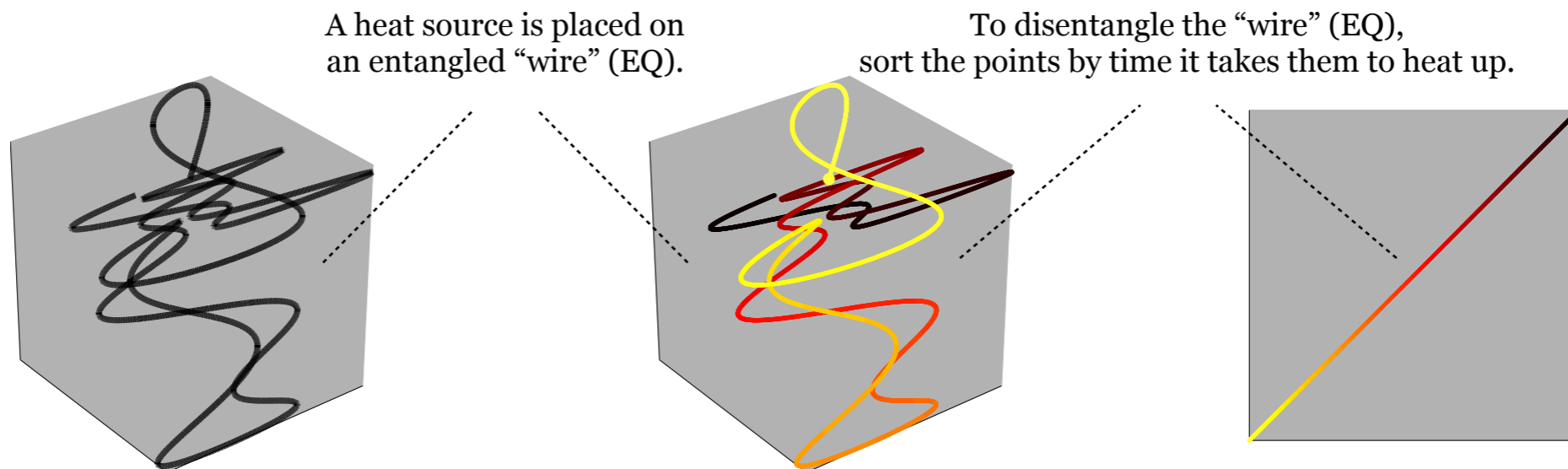


The **scalar fields used in averaging** were chosen regardless of dynamics, so they yield a **high-dimensional space**.

The dimension of EQ can be **very low**, if the dynamics is simple, e.g., when there is only a **single gyre**, or a **single mixing region**.

Diffusion Maps:

[Coifman, Lafon, ACHA, 2006]



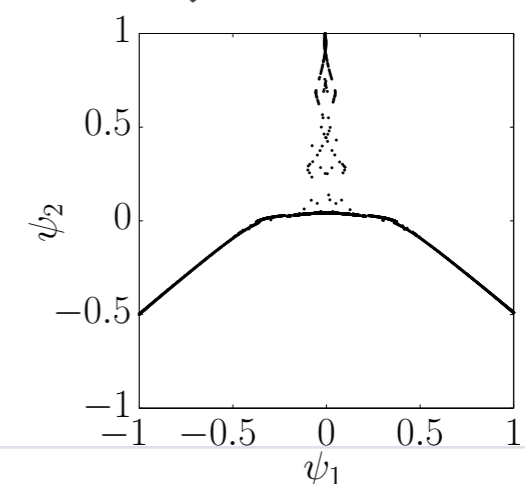
Implementation requires only **deterministic matrix computations**.

Topology and geometry are preserved, e.g., a continuous line is still a line, but the **number of coordinates is greatly reduced**.

$$(p, T) \mapsto \begin{bmatrix} \tilde{f}_1(p, T) \\ \tilde{f}_2(p, T) \\ \vdots \end{bmatrix} \mapsto \begin{bmatrix} \Psi_1(p, T) \\ \Psi_2(p, T) \\ \vdots \end{bmatrix}$$

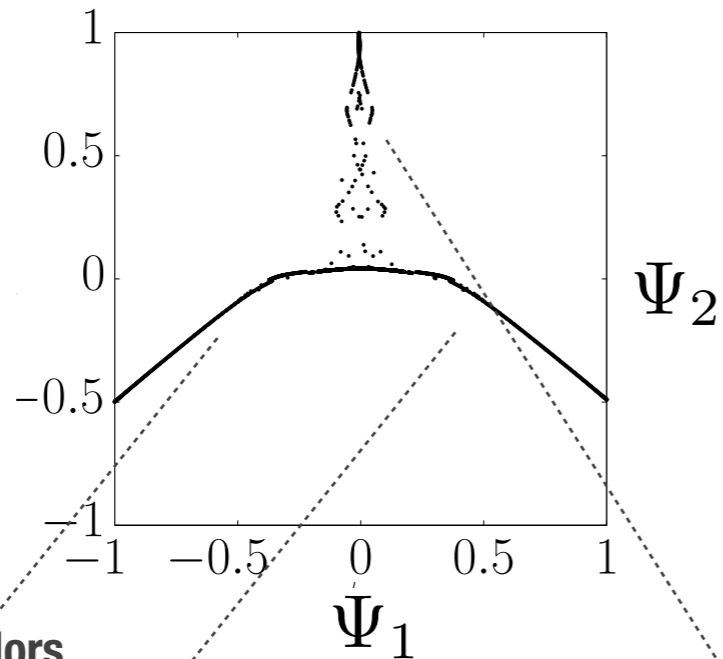
Tracer paths Averaged fields Diffusion Coordinates

EQ: Diffusion Coord.

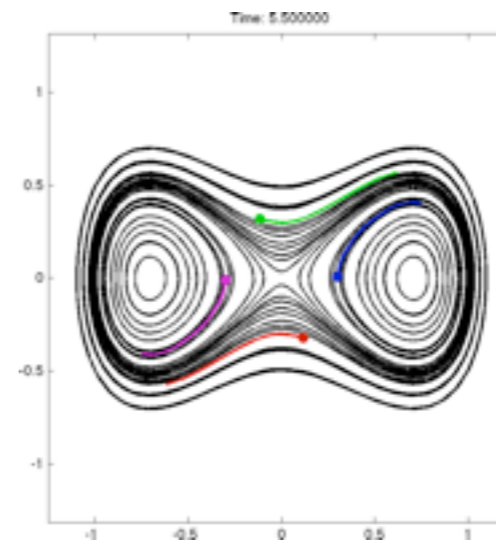


Coloring the state space by values of dominant diffusion coordinates reveals large scale features.

EQ: Diffusion Coordinates as axes

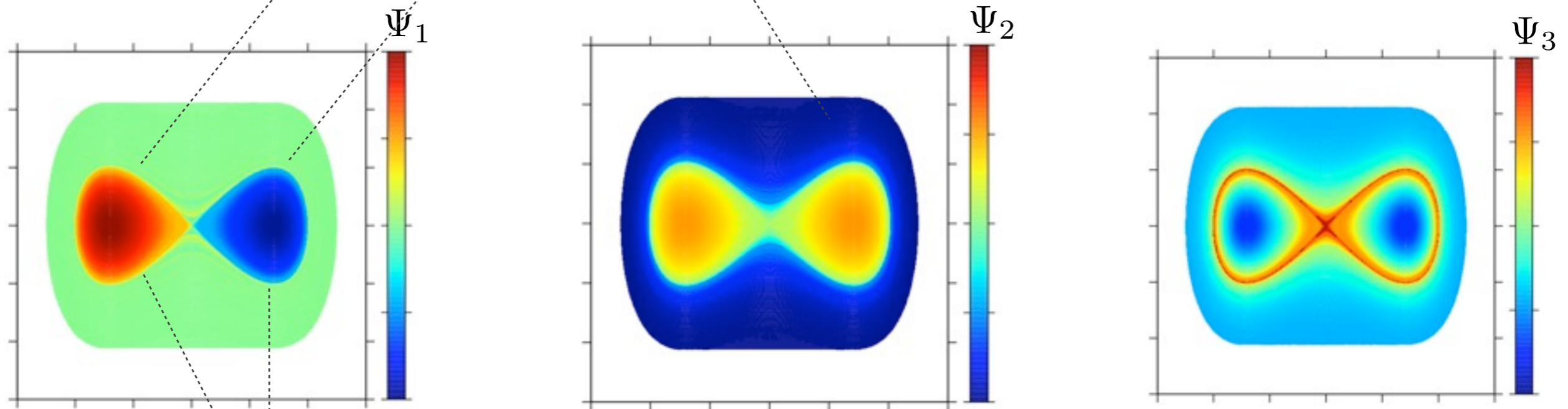


State Portrait



Number of diffusion coordinates depends on complexity of dynamics, **not dimension of the state space.**

Diffusion Coordinates as colors



Different colors indicate there is no material transport between regions.

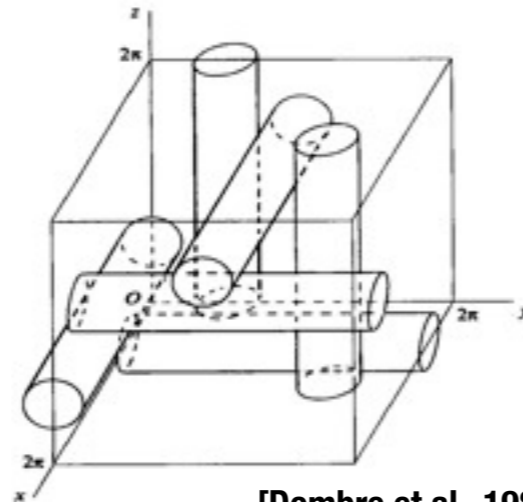
Coordinates of higher order distinguish between finer features.

Steady 3D flow: ABC system.

$$\begin{bmatrix} \dot{x} \\ \dot{y} \\ \dot{z} \end{bmatrix} = \begin{bmatrix} A \sin z + C \cos y \\ B \sin x + A \cos z \\ C \sin y + B \cos x \end{bmatrix}$$

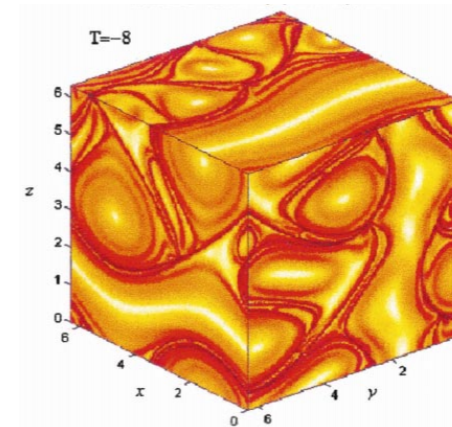
$$A^2 = 3, \quad B^2 = 2, \quad C^2 = 1$$

Analytic



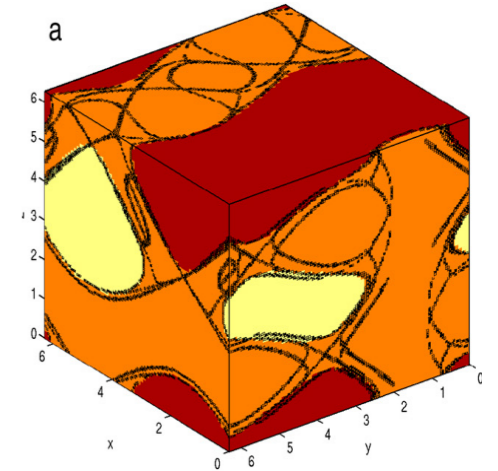
[Dombre et al., 1986]

LCS FTLE



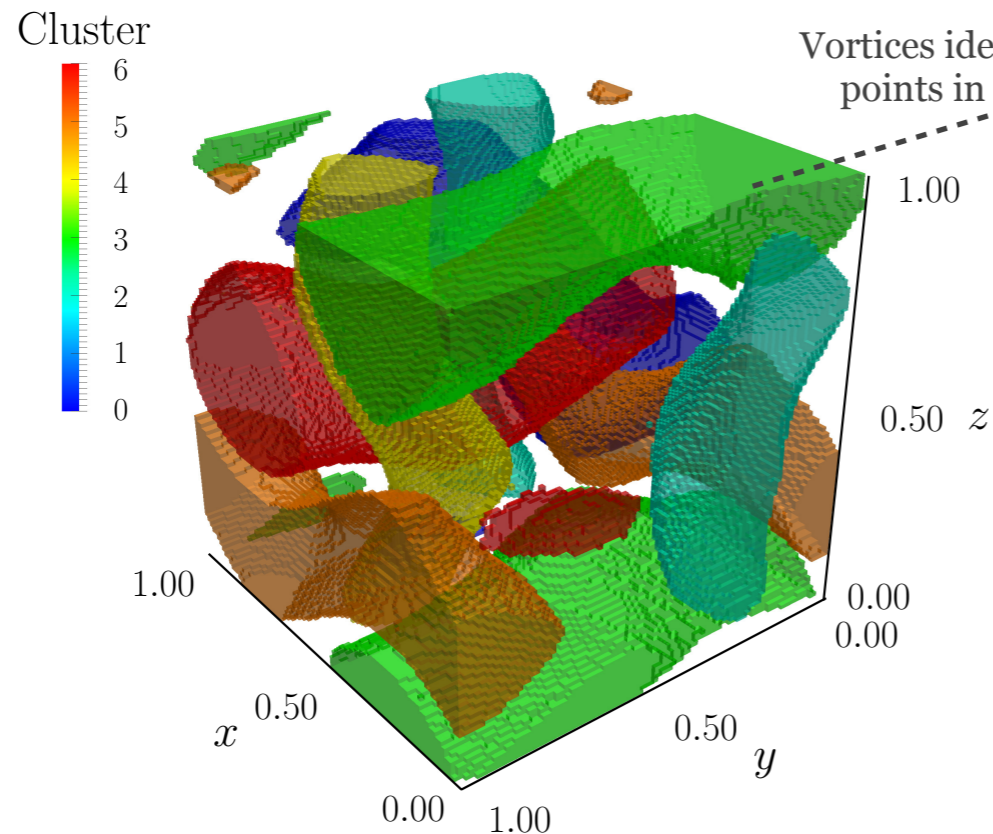
[Haller, 2001]

Almost-invariant sets



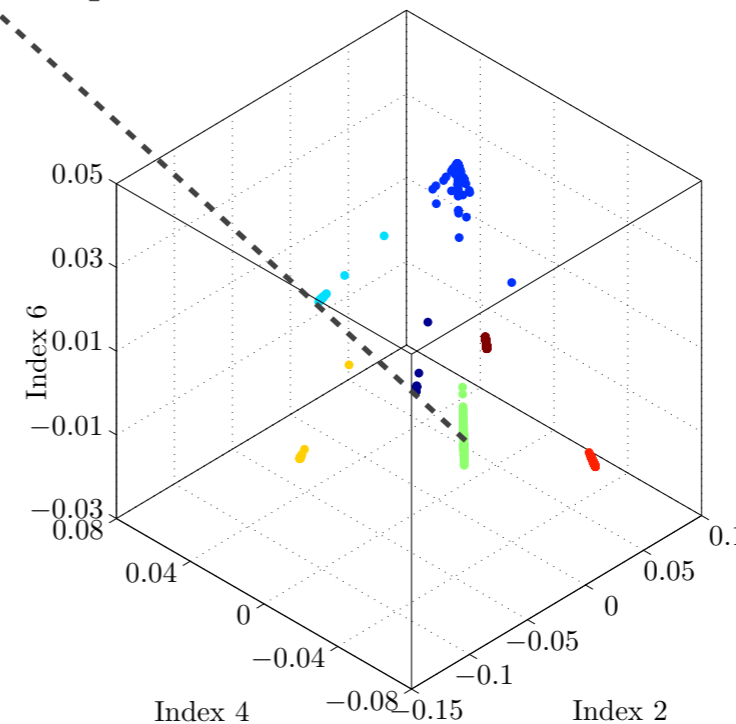
[Froyland et al., 2009]

State space coloring

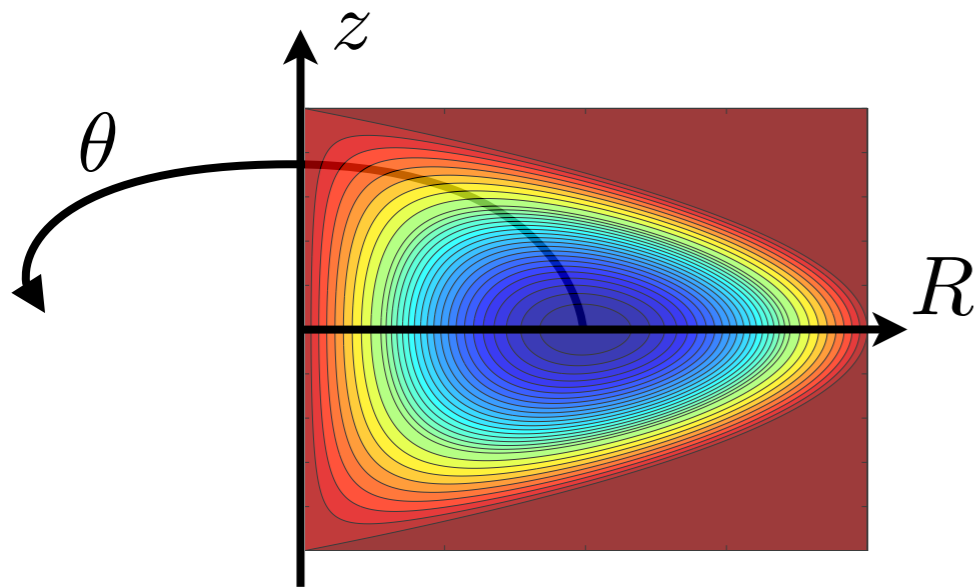


EQ in Diffusion Coordinates

Vortices identified as clusters of points in diff. coord. space.



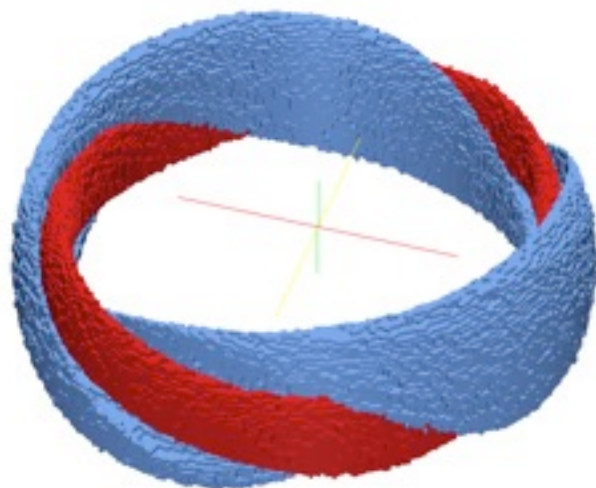
Periodic 3D+1 flow: unsteady Hill's ring vortex



$$\begin{aligned}
 \begin{bmatrix} \dot{R} \\ \dot{z} \\ \dot{\theta} \end{bmatrix} &= \begin{bmatrix} \text{Hill's Vortex} \\ 2Rz \\ 1 - 4R - z^2 \\ \text{Steady Swirl} \\ \frac{c}{2R} \end{bmatrix} + \varepsilon \begin{bmatrix} \text{Unsteady Perturbation} \\ \sqrt{2R} \sin \theta \\ \frac{z}{\sqrt{2R}} \sin \theta \\ 2 \cos \theta \end{bmatrix} \sin 2\pi t \\
 & \quad (R, z, \theta) \in \mathbb{R}^+ \times \mathbb{R} \times \mathbb{T}
 \end{aligned}$$

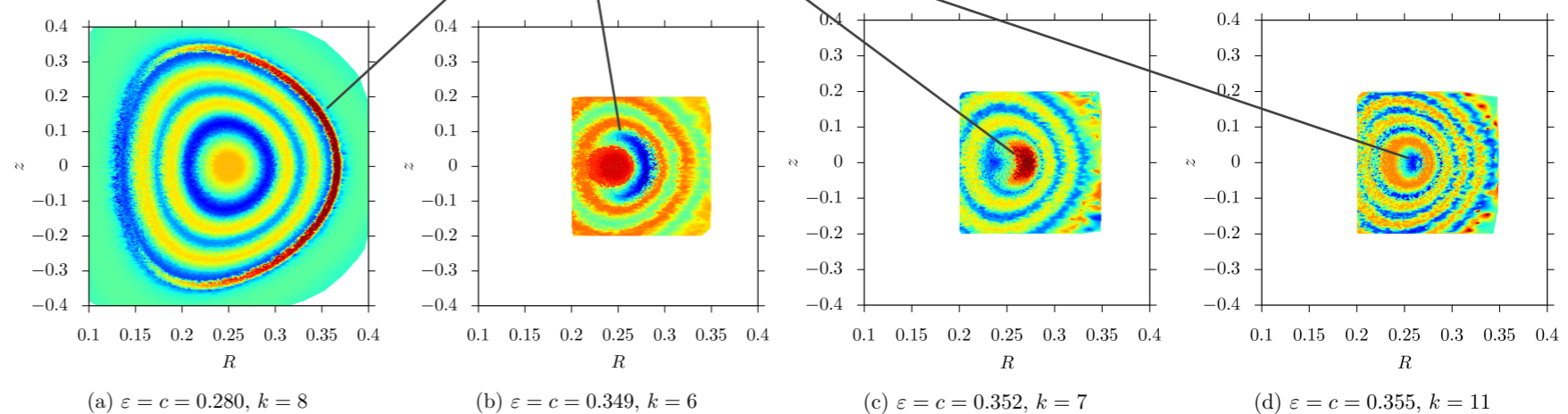
The unsteady perturbation splits the ring vortex into a primary core vortex and a secondary companion vortex.

Invariant tori in Poincaré section isolated using the ergodic quotient:



New bifurcation identified:

A crescent shaped secondary vortex appears and disappears

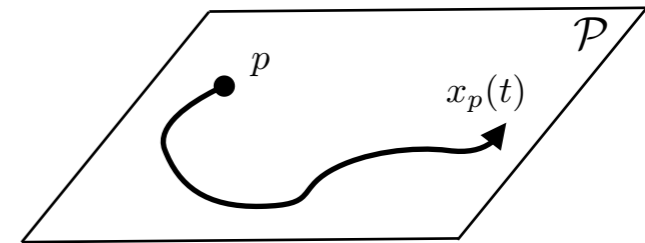


Both analyses use Lagrangian averaging, but applied to different fields.

Lagrangian trajectory:

$$\dot{x}_p = u(t, x_p), \quad x_p(0) = p$$

$$(p, t) \mapsto x_p(t)$$



Lagrangian average:

$$\tilde{f}(p, T) := \frac{1}{T} \int_0^T f(\tau, x_p(\tau)) d\tau$$

Initial condition

Averaging Interval

Choice of the field(s)
to be averaged

I. Ergodic Quotient: Coherent Structures

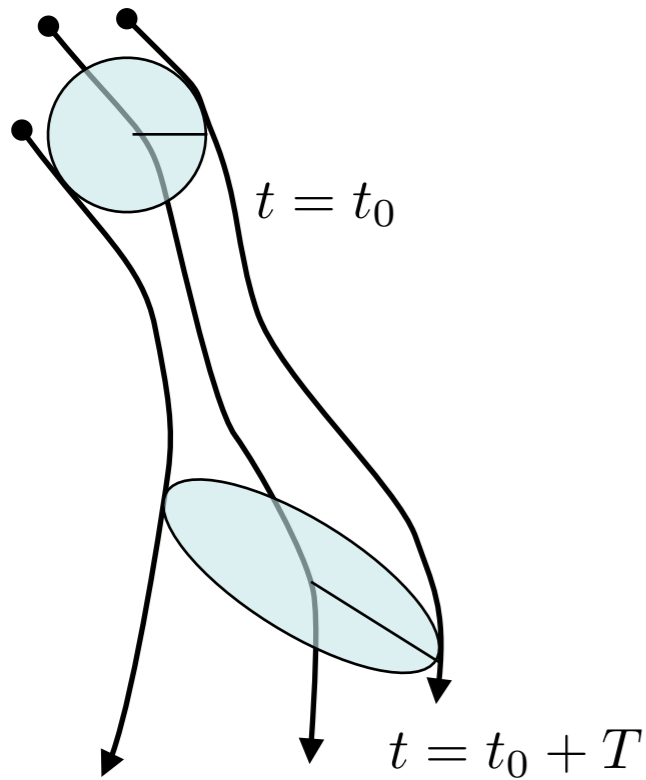
A (large) number of **stationary scalar fields**, related to the domain, not dynamics, e.g., spatial Fourier harmonics.

II. Mesochronic Analysis: Material Deformation

Fluid velocity field:
a single non-stationary vector field.

$$f(t, x) = u(t, x)$$

Linear deformation of the material is the basis for several flow analysis techniques.



Maximal Finite-Time Lyapunov Exponents (FTLE):

Detect only the maximal **magnitude** of deformation, **not its character** (e.g., shear, rotation).

Analysis often depends on locally maximising curves as barriers to transport.

Mesochronic Analysis:

Classifies deformation based on its **character**, not its magnitude.

Our focus is on the Flow Map:

$$\dot{x}_p = f(t, x_p), \quad x_p(0) = p$$

Flow map assigns final position to initial.

$$p \rightarrow \Phi(p, T) = x_p(T)$$

$$T \rightarrow 0^+$$

Instantaneous analysis is equivalent to vector field analysis.

In unsteady flows, instantaneous analysis gives poor predictions. Move to finite times.

$$T > 0$$

Deformation by the Flow Map is captured by the Jacobian of trajectory averages of the velocity field.

Flow map can be interpreted as a Lagrangian **average of the velocity field**.

Flow map $\Phi(p, T) = p + \int_0^T f(\tau, x_p(\tau)) d\tau$

Mesochronic (=Time-Averaged) velocity field $\tilde{f}(p, T) = \frac{1}{T} \int_0^T f(\tau, x_p(\tau)) d\tau$

$$\Phi(p, T) = p + T \tilde{f}(p, T)$$

Mesochronic Jacobian captures the linear deformation by the flow.

$$J_{\tilde{f}}(p, T) = \frac{J_{\Phi}(p, T) - \text{Id}}{T} = \begin{bmatrix} \partial_1 \tilde{f}_1(p, T) & \partial_2 \tilde{f}_1(p, T) & \dots \\ \partial_1 \tilde{f}_2(p, T) & \partial_2 \tilde{f}_2(p, T) & \\ \vdots & & \ddots \end{bmatrix}$$

Locations of the eigenvalues determine the character of deformation.

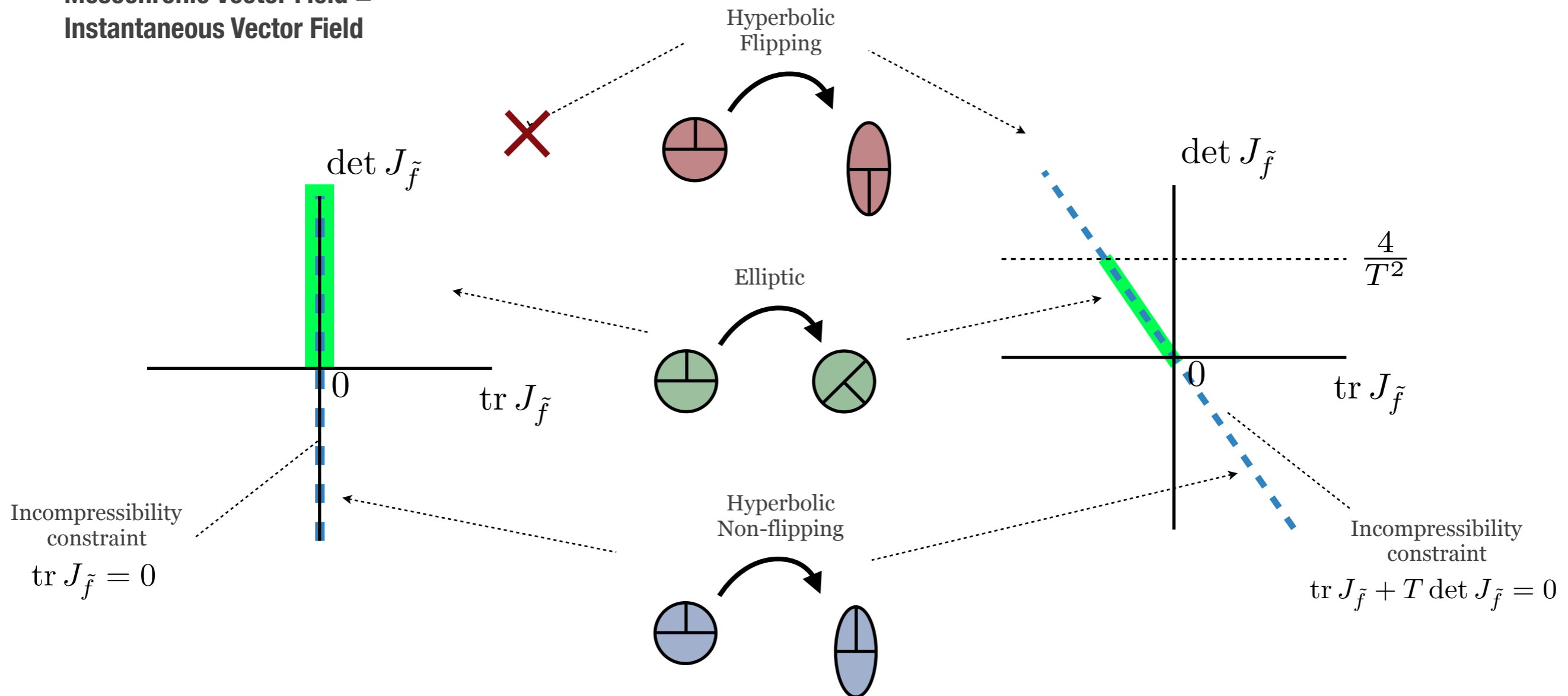
In 2D flows, a single quantity characterizes the deformation.

Okubo-Weiss: $T = 0^+$

Mesochronic Analysis: $T > 0$

Mesochronic Vector Field =
Instantaneous Vector Field

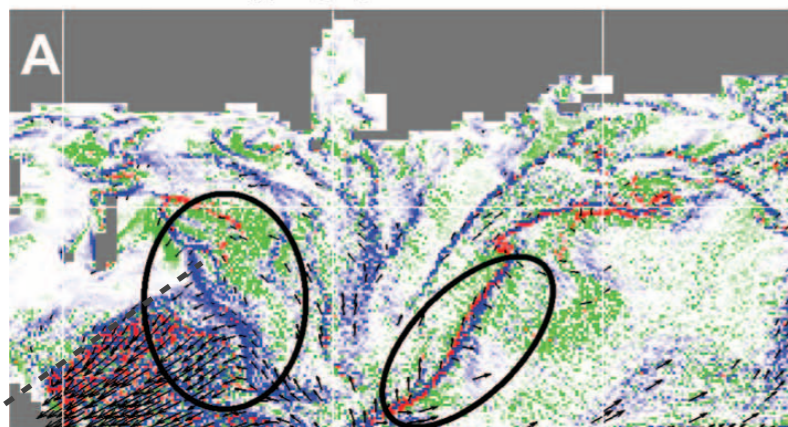
[Mezić, Loire, et al., Science, 2010]



Mesochronic analysis of 2D flows correctly detected phenomena related to the Deepwater Horizon Spill.

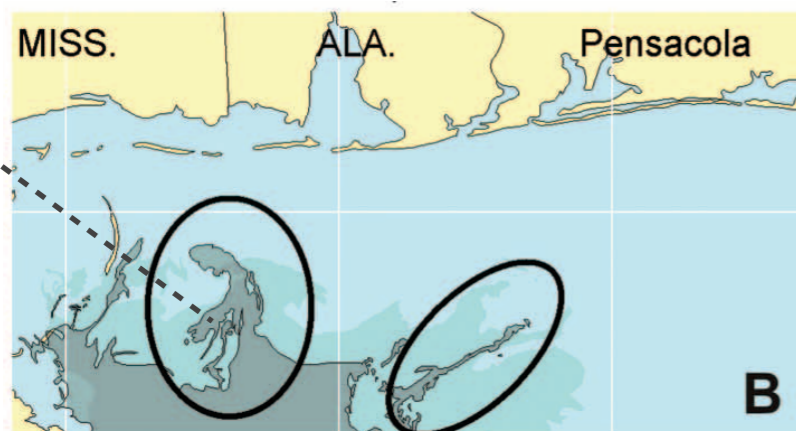
Oil slick distribution (May, 2010):

Mesochronic Classes (May 25, 2010)



Prediction

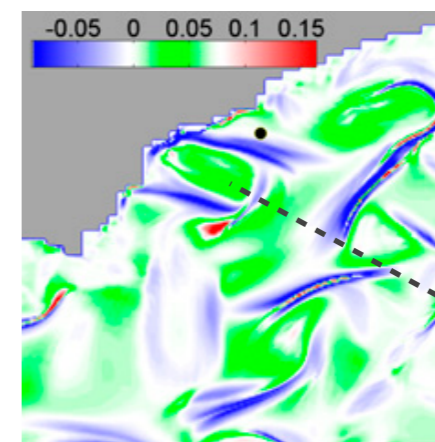
Oil Slick (May 27, 2010)



Hyperbolic deformation corresponds to jets.

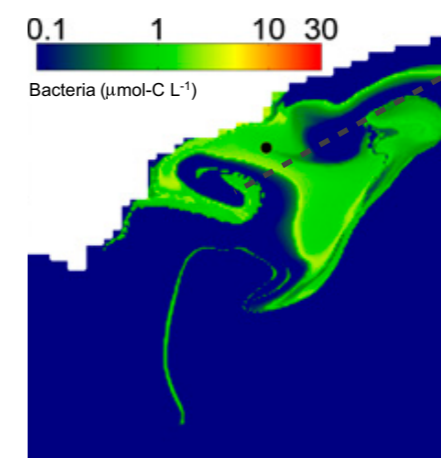
Distribution of bacteria (Jun, 2010):

Mesochronic Classes



Elliptic deformation corresponds to gyres.

Bacterial respiration

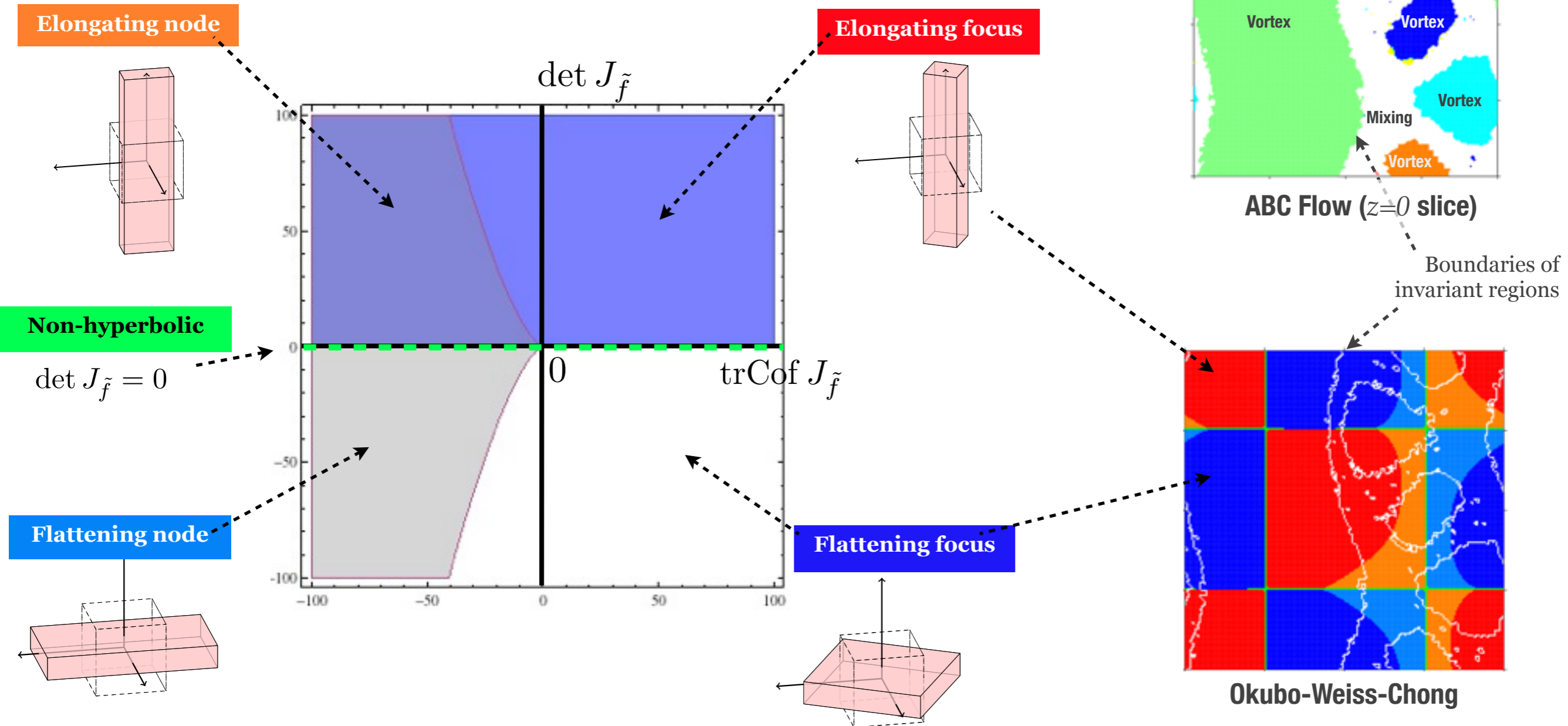


[Mezic, Loire et al., Science, 2010]

[Valentine, Mezic et al., PNAS, 2012]

In 3D flows, deformations are characterized by two quantities.

$T = 0^+$ Okubo-Weiss-Chong:

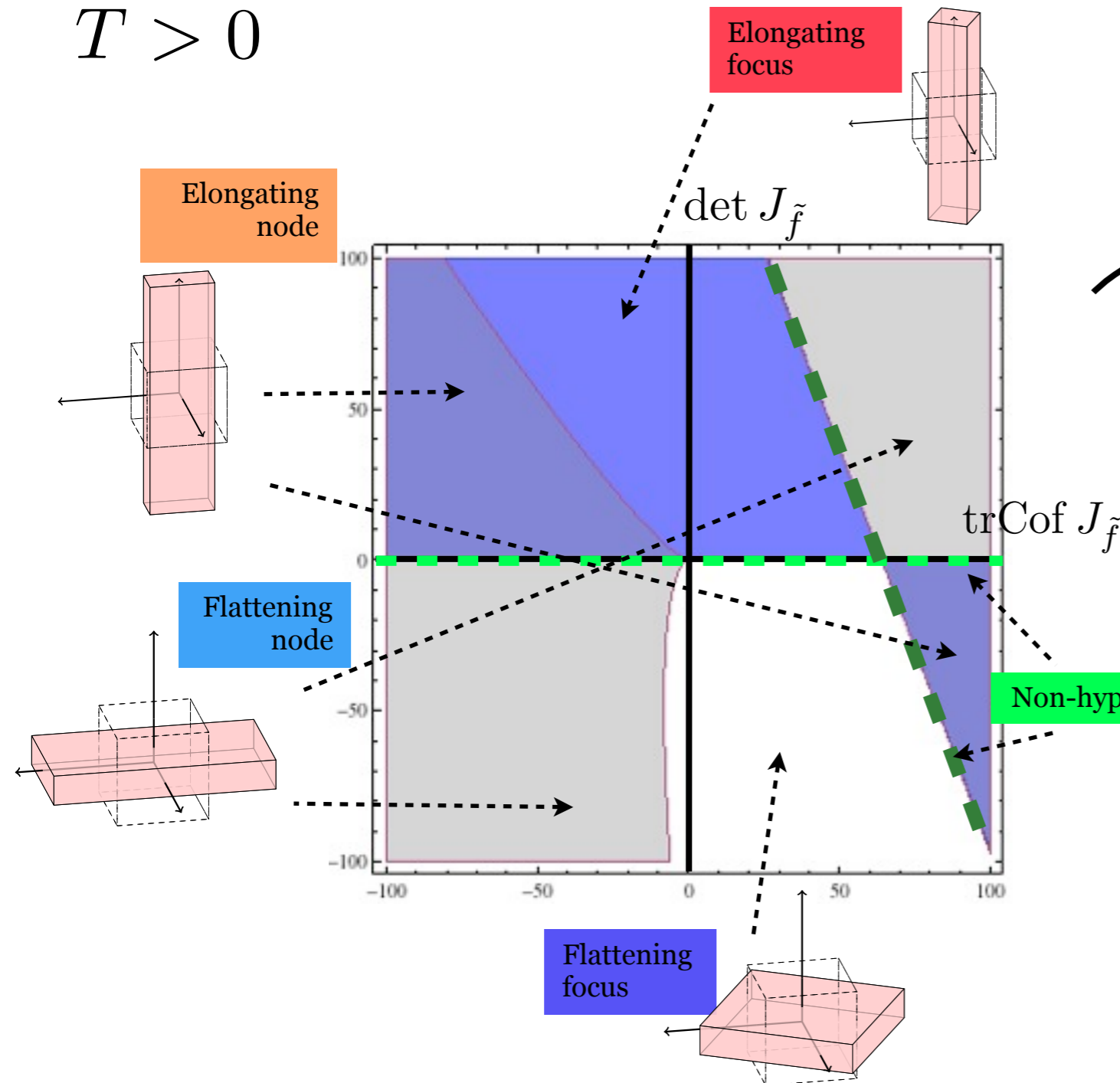


Criterion yields **non-intuitive results even for steady flows:**
boundaries do not match understanding of invariant structures.

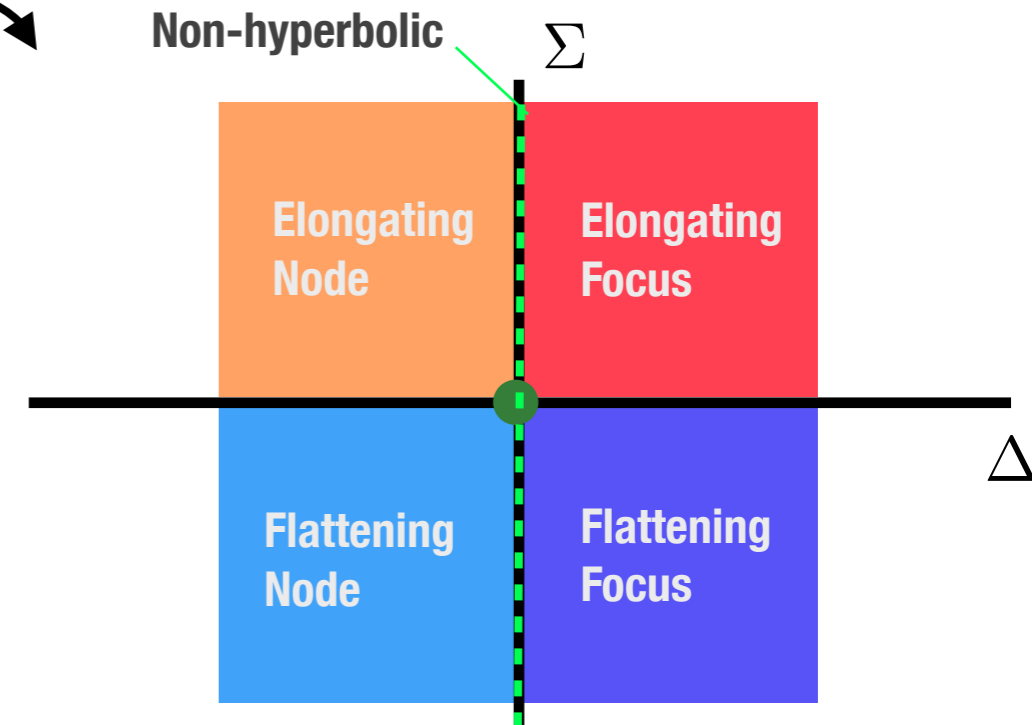
Mesochronic deformation classes can be identified by signs of two independent parameters.

$$T > 0$$

Introduce two new quantities $\Sigma \Delta$ that separate hyperbolic classes:



Non-hyperbolic

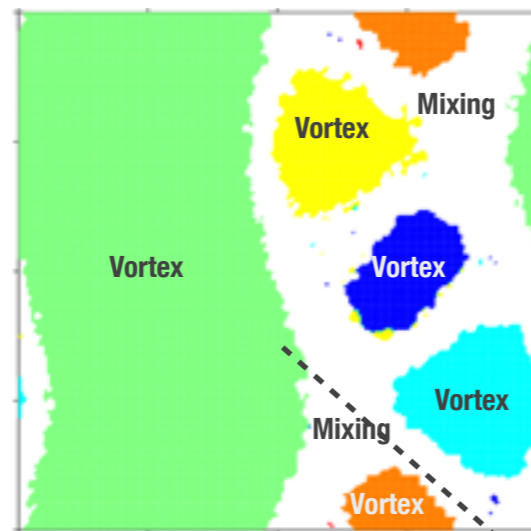
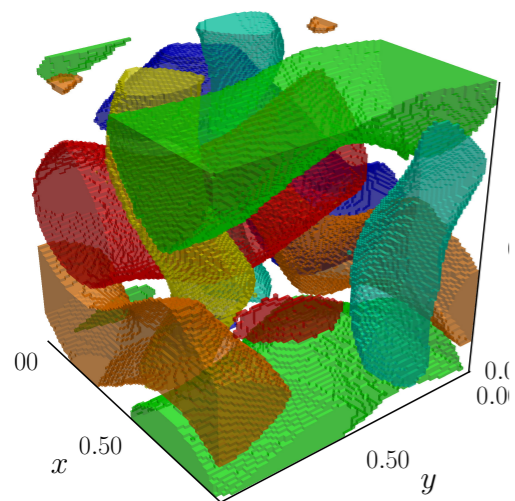


Incompressibility:

$$\text{tr } J_{\tilde{f}} + T \text{trCof } J_{\tilde{f}} + T^2 \det J_{\tilde{f}} = 0$$

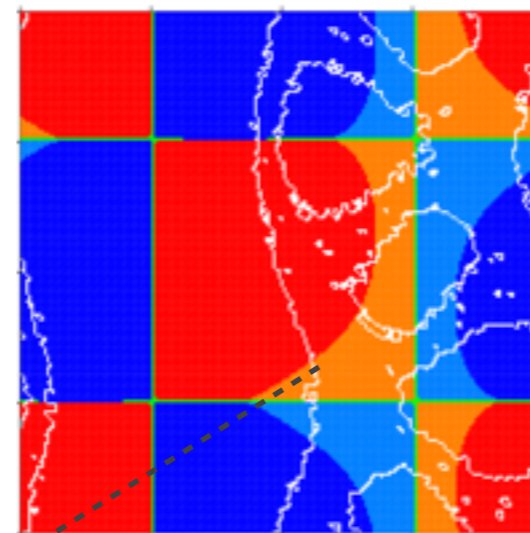
Analysis of ABC flow structures matches our intuition.

Invariant sets ($z=0$ slice)



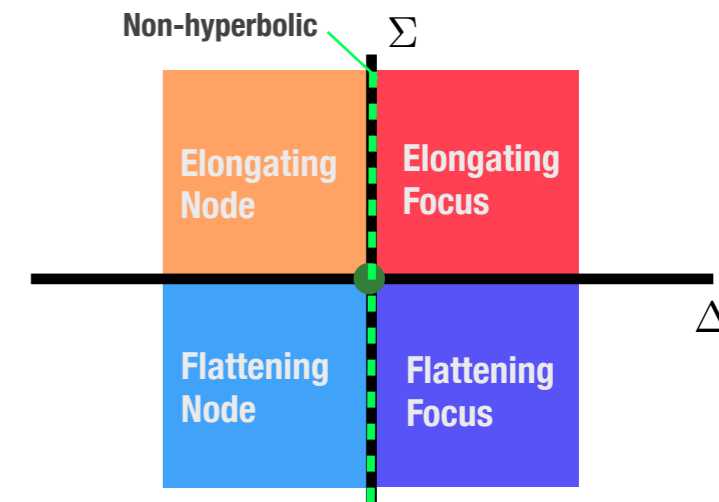
Boundaries of invariant regions

Okubo-Weiss-Chong

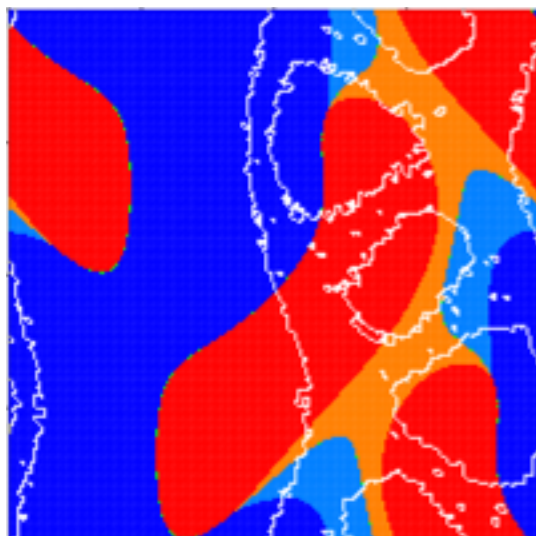


$T=0^+$

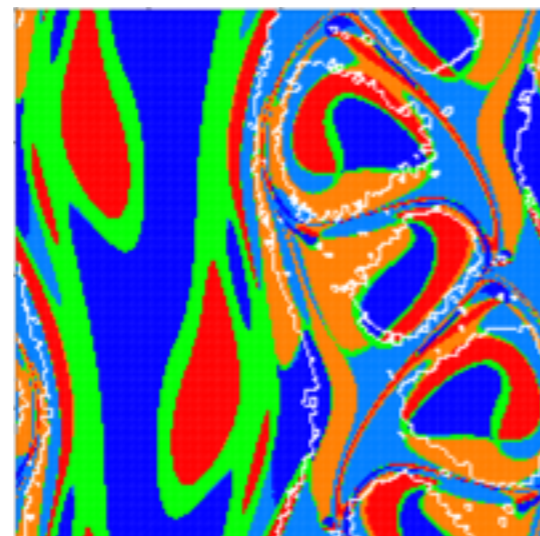
Mesochronic Classes



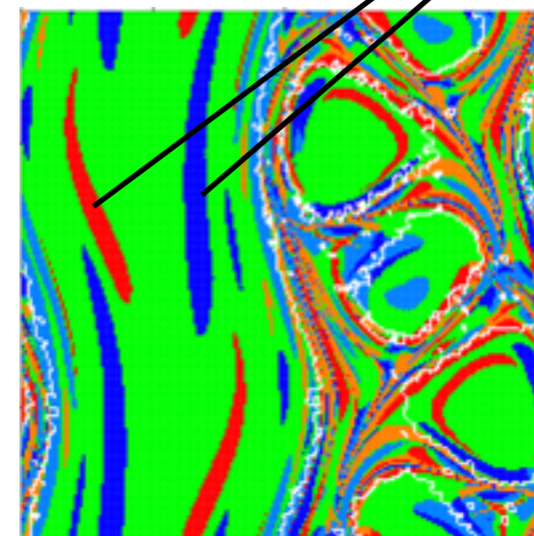
Hyperbolicity dominates at short time scales.



$T=1$

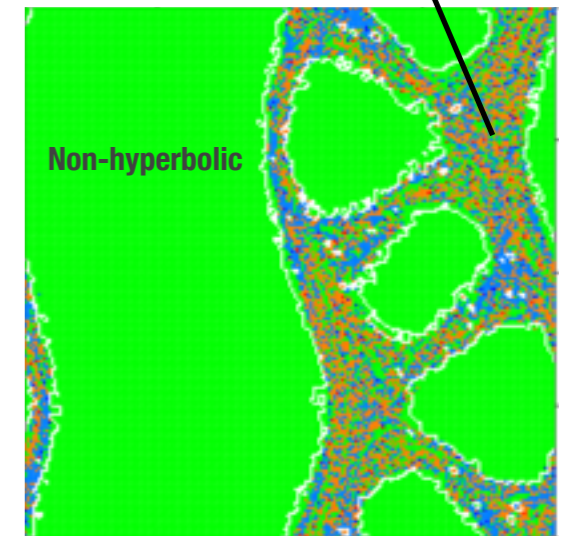


$T=5$



$T=10$

Mixture: non-hyperbolic, flattening and elongating



$T=50$

Near-future developments:

Understanding parametrization: how does **change in initial and final averaging time** affect our interpretation of results.

Techniques will be converted into user-friendly code and **shared within the collaboration.**

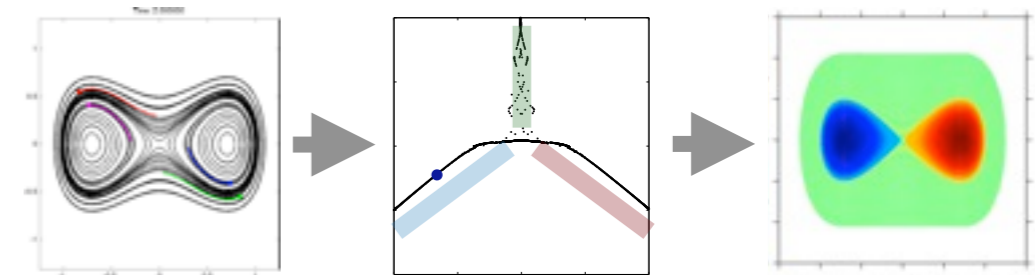
Applying the techniques to **physical flows**: see Drew Poje's talk.

Ergodic quotient: Identification of coherent structures

Budišić and Mezić, *Geometry of the ergodic quotient reveals coherent structures in flows*, **Physica D**, 241, (2012).

Budišić, Mohr, and Mezić, *Applied Koopmanism*, **Chaos** 22, (2012).

+1 in preparation



Mesochronic analysis: Character of material deformation

Mezić, Loire, et al., *A New Mixing Diagnostic and Gulf Oil Spill Movement*, **Science** 330, (2010).

Valentine, Mezić, et al., *Dynamic autoinoculation and the microbial ecology of a deep water hydrocarbon irruption*, **PNAS** 109, (2012).

+2 in preparation

